Investigation of hydrogen and oxygen impurities in alkali metals

R. P. Layton* and C. P. Flynn
Physics Department and Materials Research Laboratory, University of Illinois at Urbana-Champaign, Urbana, Illinois 61801
(Received 25 October 1978)

Hydrogen and oxygen impurities in alkali-metal host lattices have been investigated by means of residual-resistance and optical-absorption ($5 < \hbar\omega < 12$ eV) measurements. It is shown that hydrogen and oxygen probably occupy interstitial sites in alkali-metal hosts, much as in transition metals. A specific signature of this site occupancy is observed in the optical spectra.

I. INTRODUCTION

The properties of hydrides and of hydrogen impurities in metals have attracted a good deal of attention in recent years. Most of the work has concerned transition-metal hydrides or more dilute hydrogen solutions in transition-metal hosts.[1,2] These systems possess both practical and fundamental importance. Much less work has appeared concerning the behavior of hydrogen in the host lattices of the simpler alkali metals, although the properties of alkali hydrides themselves have been the subject of some investigation.[3] To our knowledge, the *dilute* solutions of hydrogen in alkali metals have not previously been examined. The present paper reports some optical and transport measurements on alkali-metal–hydrogen alloys that give insight into the structure of hydrogen in these solvents. Similar measurements have been performed on alkali-metal alloys with oxygen and tellurium also, to provide a useful comparison with the hydrogen results.

In our initial approach to this problem we were misled by recent results obtained by our group for other impurities in alkali metals.[4] Halogens, chalcogens, and other atomic species enter alkali hosts as *negative ions* on substitutional sites. They are screened to electrical neutrality by conduction electrons *repelled* from the ionic impurity center, and this local reduction of electron density leaves the ion rather decoupled from the conduction band. A number of properties, including spin-flip scattering of conduction electrons, residual resistance, impurity diamagnetism, and the impurity excitation spectrum confirm the basic accuracy of these structural assignments.[4]

Hydrogen in alkali metals also presents an interesting problem from the tight-binding viewpoint, since H orbitals fall at −13.6 eV while alkali orbitals are typically near −5 eV. This indication that charge transfer to substitutional H may be important is borne out by the fact that H maintains an affinity of 0.73 eV for creation of H^-, even in vacuum. Accordingly, substitutional H in an alkali metal may well exist in part as H^-, in the $1s^2$ configuration. The opportunity to study this interestingly correlation-sensitive system failed to emerge in practice because our sample preparation techniques were unable to produce substitutional hydrogen impurities. We find strong indications that both H and O occupy *interstitial* sites in bcc alkali metals, just as in transitional bcc metals. Apparently, also, the lack of free volume associated with cell occupancy inhibits the occurrence of charge transfer to interstitials, since the present observations show no indication of charge transfer structures.

In what follows, the equipment and sample preparation methods employed in this work are first outlined in Sec. II. The observed resistance and optical results are presented in Sec. III, and the accumulated information is then discussed in Sec. IV.

II. EXPERIMENTAL DETAILS

A. Apparatus

Optical measurements were made by comparing the light intensities transmitted through twin, thin-film samples, one pure and one doped with impurity. The way in which these were prepared is discussed in Sec. II B below. In practice, the twin samples contained equal area densities of host atoms. The two transmitted beams were chopped at differing frequencies and detected by a single photomultiplier whose output passed through filtering circuits to an Ithaco R300 ratiometric lock-in system. The Ithaco output was fed through a logarithmic amplifier to a chart recorder whose reading measured the impurity effects alone, assuming that the samples were perfectly balanced. Details of this technique are described elsewhere.[5] The impurity spectra presented below give the absolute absorption cross section μ per impurity, as determined by these methods.[5]

The light beams passing through the sample was obtained from a homemade vacuum ultraviolet monochromator fed by a hydrogen lamp. The

only materials intersecting the light beam between this source and the sodium salicylate phosphor on the photomultiplier tube were two 1-mm-thick LiF crystals, one acting as the sample substrate and the second as a window of the vacuum chamber in which the samples were prepared and measured. The optical cutoff of these LiF crystals near 12 eV proved to be a serious problem in the present work, but alternative methods for precise alloy preparation in vacuum are lacking at the present time. No deterioration of even the most reactive alkali-metal samples was detected over the course of hours in the 10^{-7}-Torr environment of the bell jar. In part, this is doubtless due to the liquid He and N_2 Dewars surrounding the samples; the cryopumping must improve the effective vacuum in the sample neighborhood by several orders of magnitude. Details of the equipment and the electrode arrangments used for resistance measurements will be found in other publications.[6]

B. Sample preparation

Dilute alloys of alkali metals containing H impurities do not seem to have been prepared before. Alkali hydride films are normally made by allowing H_2 gas to react with alkali-metal films at room temperature.[3] This method offers no possibility for the preparation of dilute samples. The alternative method we developed was at least partly effective. It made use of an atomic hydrogen beam and an alkali-metal evaporation stream codepositing onto a substrate held at liquid-He temperature. With this system we were able to observe residual resistivities proportional to the H density, and proportional changes of optical spectra that had no relationship to the hydride compound spectra. These effects are consistent with the presence of H in solution as a random impurity. In addition, these changes were wholly absent when a molecular H_2 beam replaced the atomic H beam.

In its final form the atomic hydrogen source used in this work was a development of that described by Eisenstadt.[7] It is shown in Fig. 1. A stream of H_2 is dissociated inside a W tube held at high temperature, and allowed to escape through a small hole in the tube wall facing the substrate. The dissociation is facilitated by low H_2 pressure, by the catalyzing effect of the W surface, and by the very high temperatures. In practice the W tube operated near 2700 K by resistance heating.

The filament itself, shown in Fig. 1, was constructed from a single length of tungsten rod by the Materials Research Laboratory machine shop using an electric discharge cutter. It consists of a thin-walled section, $\frac{1}{16}$-in.-o.d. with 0.011-in. walls and a 0.012-in. diam orifice, connected to

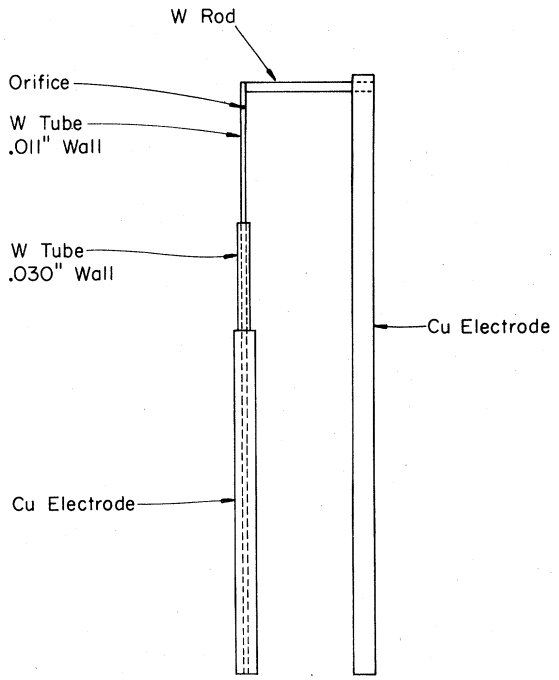

FIG. 1. Atomic hydrogen source.

a $\frac{1}{8}$-in.-o.d. section with 0.030-in. walls. The large end was electron-beam welded to a copper electrode which has a $\frac{1}{16}$-in. hole drilled through its entire length. The thin-walled filament was enlarged at its free end to facilitate the electron-beam welding of the filament to the solid tungsten rod cross piece. This rod in turn was beam welded to the second copper electrode. Two heavier pieces of tungsten at each end of the filament helped to thermally isolate it from the copper parts of the system. The copper conductors themselves were made of oxygen-free high-conductivity copper and were annealed to relieve the stresses produced by thermal expansion when the filament was heated. Water-cooled copper clamps were attached to the end of the copper conductors to hold them in place and to provide electrical contact.

To produce atomic hydrogen, the filament was heated to 2700 K by resistance heating while H_2 was delivered to the tungsten tube through the hollow copper electrode. A voltage drop of 2.1 V across the assembly at a current 84 A was needed to achieve this temperature. A water-cooled copper shield enclosed the filament to reduce the radiant heat that reached the Dewar and sample substrate.

The design described above worked quite effectively throughout repeated cycles of heating and cooling the filament. When the filament was slowly brought to the desired temperature the annealed

copper conductors absorbed the thermal stresses in the system well enough to prevent the thin-walled W tube from bending irreversibly or breaking. Most of the energy fed into the system was radiated by the filament and very little carried away by the water-cooled copper electrodes or the copper shield.

During actual sample preparation, the filament was brought into stable operation with the alkali-metal evaporation simultaneously established at a level chosen to create the desired alloy composition. Shutters were then opened to expose the cold substrate to the two beams, and left open until the appropriate film thickness was reached. Very similar methods were used to prepare alloys with oxygen doping, except that the filament was operated at room temperature for oxygen. Tellurium alloys were made using two evaporation beams controlled independently.

C. Beam calibration

The alkali evaporation rate was monitored by means of a quartz crystal placed in the beam outside the direct path to the substrate. It was calibrated directly by auxilliary measurements in which the frequency shift of a quartz crystal fixed on the sample substrate was compared with that of the monitor crystal. Similar procedures were employed to determine Te densities. For O_2, the beam density was established as a function of the external pressure driving the gas, again using a crystal fixed to the substrate. It was assumed that O_2 has a sticking factor of unity on the quartz crystal at liquid-He temperature.

Greater difficulties occurred in calibrating the hydrogen beam. The thermal coupling between the liquid-He Dewar and the quartz crystal, which was directly clamped to the Cu sample holder, could not dissipate the radiant heat from the H source while maintaining the crystal at sufficiently low temperature for H to stick (although Ne did stick). This problem was solved by observing the pressure decay in the gas reservoir feeding the source. Assuming that at these pressures (a few Torr) all gases are ideal, the same pressure decay for different gases corresponds to the same number of escaping molecules. The H_2 fluxes at the substrate deduced in this way from the observed decay rates and fluxes of N_2, O_2, Ne, and Ar, taken together with the observed H_2 decay rate, were mutually consistent to about 2%. In addition, the Ar and Ne deposition rates remained unaffected when the tungsten filament was heated to 2700 K. We are therefore confident that the total hydrogen flux was well established.

Two further complications enter into a precise characterization of the hydrogen deposition. The first is the ratio of molecular to atomic hydrogen in the beam leaving the filament, and the second concerns the sticking factors for the two components of the beam. In practice, the latter problem had a simple resolution. It turned out that molecular H_2 from the cold tungsten source failed to codeposit with alkali metal on the He temperature substrates. This was established by the absence of both residual resistance and optical absorption associated with the possible hydrogen impurity content of the films. On the other hand, atomic hydrogen has been found to chemisorb at 78 K on all metals and semimetals that have been studied, which include Na and K.[8,9] For this reason we assumed that the sticking probability on alkali metals at He temperature is unity, although this lacks direct experimental verification.

The remaining difficulty concerns the degree of dissociation undergone by H_2 in the tungsten filament. With the chosen filament geometry, in which H_2 must encounter the walls numerous times before escaping through the orifice, it is very likely that the W catalyst maintained the escaping beam close to thermal equilibrium at the orifice temperature. For these conditions, the degree of dissociation varies with temperature and pressure as shown in Fig. 2.[10] Under the typical operating conditions of our source, the pressure could not have been greater than 10 Torr and the effective pressure near the orifice could be much less. According to Fig. 2, then, the degree of dissociation at 2700 K must lie between 0.3 and 0.8. In practice, we took the estimate of 0.5 for the dissociation in the belief that this value is certainly accurate to within a factor of 2, and probably to within a factor of 1.5. In all cases, the filament temperature was measured using a

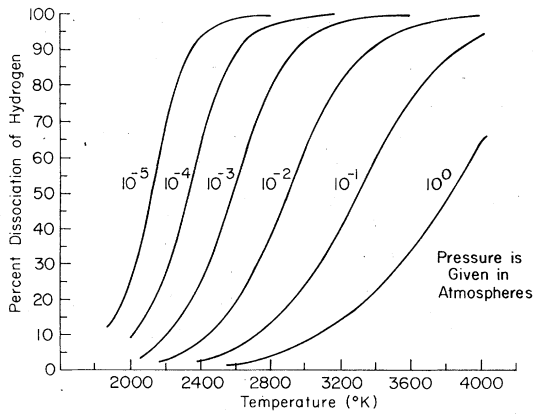

FIG. 2. Theoretical curves of percent dissociation of H_2 as a function of temperature and pressure (Ref. 12).

vanishing-filament optical pyrometer precise enough that it introduced negligible added uncertainty into the estimates of dissociation efficiency explained above.

III. RESULTS

Figure 3 shows the observed resistivities of alloy films containing oxygen dissolved in alkali metals. The measurements for Cs proved to be the most reliable, with a progressive increase in scatter apparent for lighter alkali-metal hosts. The scatter appears to be associated with chemical attach by the sample on the electrodes used for resistance measurements. These consisted principally of Ag deposited on a thin (~100 Å) layer of Al, with In used to solder into place the Cu leads required to measure sample resistance. For Na and Li the scatter became large enough to make the results unreliable, so the data reported here pertain only to K, Rb, and Cs hosts. A significant factor is that the observed resistances are quite small compared with those of other impurities. O in Cs, for example, was found to have a residual resistance ~1 $\mu\Omega$cm/at.%, which may be compared with typical impurity resistances one order of magnitude higher.[4]

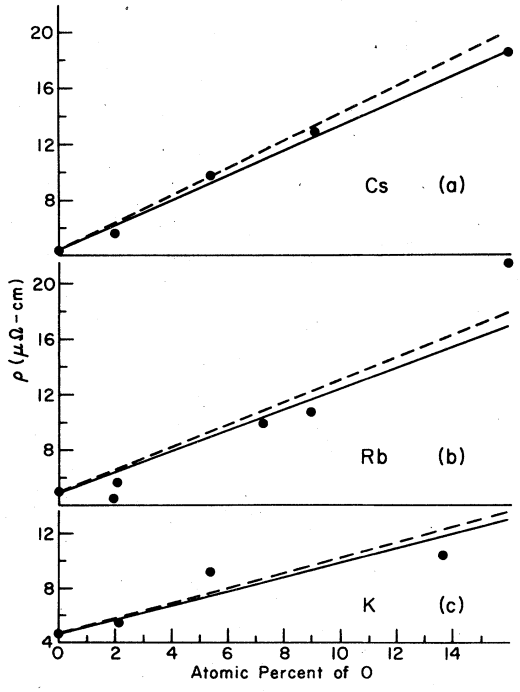

FIG. 3. Resistivity data obtained for oxygen impurities in the alkali metals Cs, Rb, and K. The solid line represents the uncorrected data while the dashed line is obtained when volume corrections are made for the presence of the impurity in the host lattice.

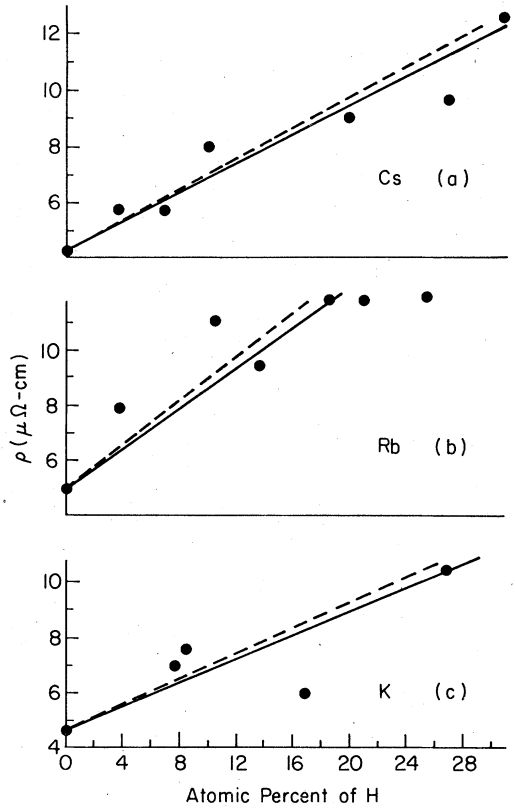

FIG. 4. Resistivity data obtained for atomic hydrogen impurities in the alkali metals Cs, Rb, and K. The solid line represents the uncorrected data while the dashed line is obtained when volume corrections are made for the presence of the impurity in the host lattice.

The impurity resistance contributed by hydrogen in K, Rb, and Cs is even smaller than that for oxygen. Figure 4 presents these data. Only for H in Cs do the data define a linear dependence of resistance on impurity concentration in a very convincing way. Even for Rb and K hosts, however, one can make a reasonable esitmate of the residual resistance. It is typically ~0.3 $\mu\Omega$cm/at.% for H in alkali metals. This value is so small that the question of sample thickness becomes important.

In order to determine the actual impurity resistance is it necessary to know the film thickness and hence the partial molar impurity volume. These quantities are not available in the literature. Reasonable esitmates can nevertheless be made. It will emerge that both O and H must occupy interstitial sites in the alkali metals. Experience with interstitials in bcc transition metals has shown that H typically occupies ~30% of one atomic volume and O perhaps 70%. The alkali lattices are, of course, more open structures, and

TABLE I. Residual resistances of H and O in $\mu\Omega$ cm/at.% for K, Rb, and Cs hosts. Possible systematic errors of ±50% in sample composition for H are not included in the stated uncertainties.

	H	O
K	$0.2_5 \pm 0.1$	0.6 ± 0.1
Rb	0.4 ± 0.1	0.8 ± 0.1
Cs	$0.3_0 \pm 0.0_5$	1.0 ± 0.1

smaller fractional volumes are to be expected. In the absence of precise information we have made the estimates of $20 \pm 10\%$ for H and $50 \pm 30\%$ for O, relying on the generous uncertainties to obtain reliable ranges. With these volumes one obtains the residual resistivities displayed in Table I for H and O in K, Rb, and Cs. The uncertainties presented there include the volume uncertainties quoted above. The broken lines in Figs. 3 and 4 show how the volume effect changes the solid lines through the data. This effect is evidently not large. The values given for H in Table I do not include the uncertainty in the absolute H concentration which may, realistically, amount to a factor of 1.5.

Optical spectra were obtained for many of the alloys discussed above. The accessible spectral range of ~5–12 eV was restricted by the metallic film transmissivity at low energy and by the LiF cutoff at high photon energy. A significant feature of the observed impurity spectra was their lack of recognizable similarity to hydride and oxide spectra of the related compounds.[3,11] Together with the resistivity data, which establish that impurities *were* introduced into solution, the optical data provide evidence that the impurities did *not* accrete into local hydride or oxide precipitates. To illustrate this point, the absorption per impurity atom for several different concentrations of H in K is presented in Fig. 5(a). The data are normalized to give the absorption *per impurity atom*. The peaks above 5 eV of the compound spectrum shown in Fig. 5(b) are absent from the impurity spectrum. In no case did H or O in any alkali host give optical absorption resembling that of the salt. These observations appear to indicate that the sample preparation methods employed here were effective in providing dilute alloys rather than compounds.

Apart from two specific phenomena, the optical results proved somewhat featureless. Figure 5(a) shows the type of broad structure observed in certain of the hydrogen alloy systems. The absorption μ *per impurity atom* reproduces quite well in the different dilute alloys, although the amplitude of the structure is small. Residual host-induced effects would normally produce structure $\propto C^{-1}$ on these spectra (see, however, the case of Cs, below). We find that the dip at about 9.0 eV for H in K is shifted to about 8.2 eV for H in Rb but the spectra remain generally similar. Data for O in K and O in Rb are shown in Figs. 6 and 7. In all these cases it is clear that the optical results do probe an impurity-induced property that is not strongly affected by impurity-impurity interactions. The alkali core levels lie beyond the LiF cutoff at $\hbar\omega \gtrsim 12$ eV,[12] and the alkali spectra lack other sharp structure below these outer core

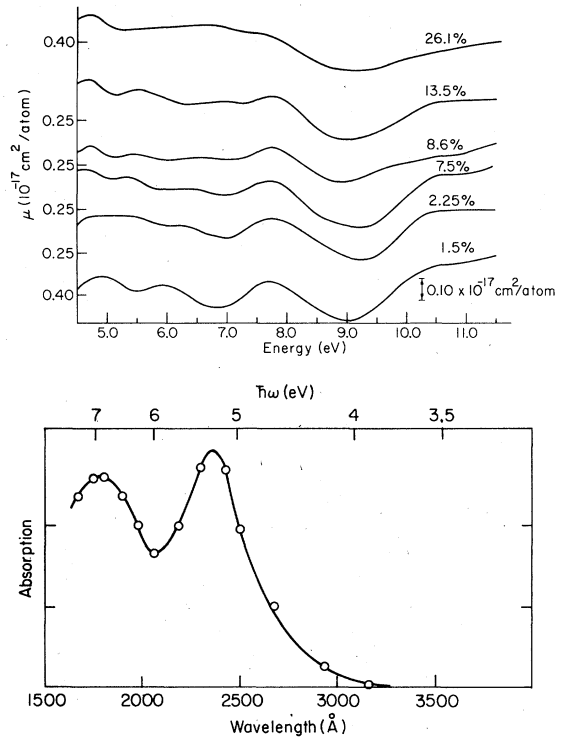

FIG. 5. (a) Absorption spectra of H in K. (b) The absorption spectrum of potassium hydride (Ref. 3).

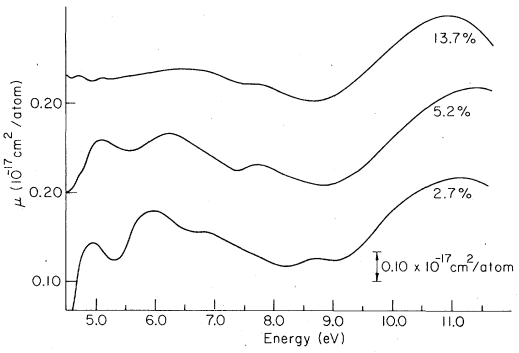

FIG. 6. Absorption spectra of oxygen in K.

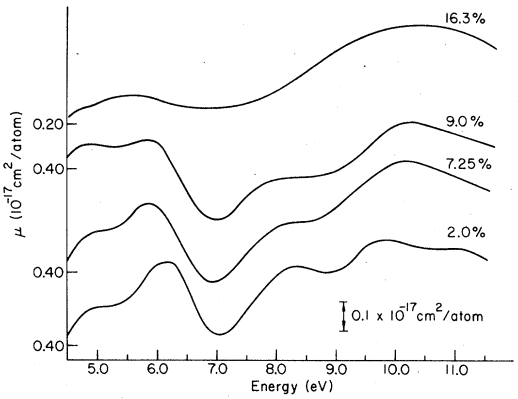

FIG. 7. Absorption spectra of oxygen in Rb.

edges.

The first of the two exceptions, in which sharp optical structure is observed in these materials, occurs for Cs-based alloys. Figure 8 shows the spectra for H in Cs and Fig. 9 shows the results for O in Cs. Note in particular the sharp peaks near the limit of the spectral scans in the region of 11.5 eV. These are explicitly absent from all other spectra. Moreover, they have amplitudes per impurity atom that reproduce reliably over a wide range of different alloys, particularly in the case of hydrogen impurities. For these reasons we identify the peaks as real impurity effects, despite their unfortunate location near the edge of the accessible spectral bandwidth. The spectrum given at the bottom of Fig. 8 was obtained when

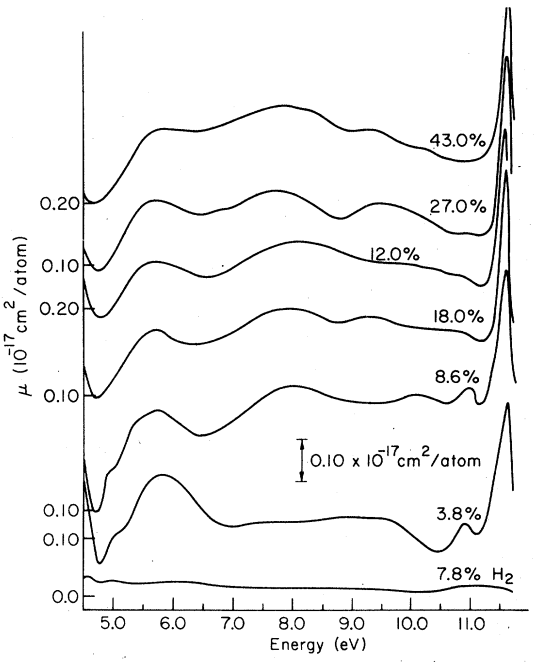

FIG. 8. Absorption spectra of H in Cs.

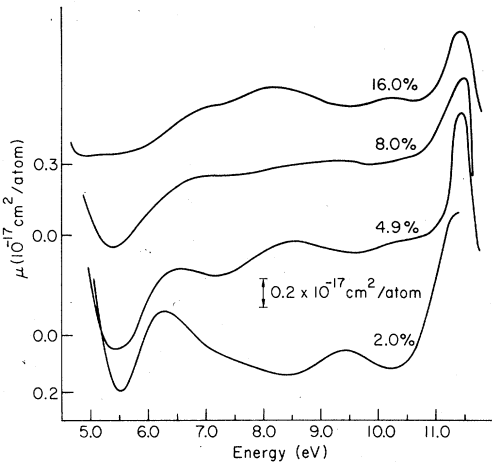

FIG. 9. Absorption spectra of oxygen in Cs.

H_2 was allowed to escape undissociated from the *cold* hydrogen source. Apparently, H_2 failed to incorporate into the alkali metal hosts, as indicated also by resistance measurements mentioned above.

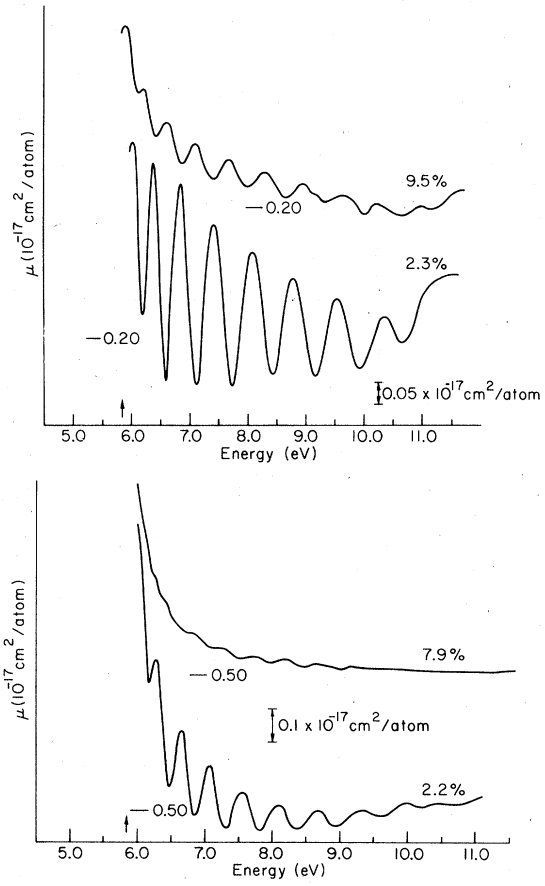

FIG. 10. (a) Absorption spectra of H in Na. (b) The absorption spectra of oxygen in Na.

This establishes that the present measurements detect only atomic H in the metallic host.

Sodium-based alloys produced the second type of notable structure observed in this work. Figure 10 displays for some H and O alloys the oscillatory differential absorption observed in the present work. Similar phenomena have been reported previously for Na alloys containing rare-gas impurities.[5] These are undoubtedly interference effects among standing optical waves in the doped and undoped films. An elementary analysis shows that the optical wavelength is smaller by a considerable factor than the value expected in vacuum. Clearly, the effect of the electron gas on the photon is rather large. These effects are not understood quantitatively at present and are the focus of ongoing experiments.

The striking contrast between the present results for H and O, and the behavior expected of substitutional impurities, is emphasized by a comparison of the oxygen data with results obtained for Te impurities. Te is an excellent charge transfer impurity, and is presumed to reside on substitutional sites because its volume is comparable with that of alkali atoms. The residual resistance in Cs is 7.4 $\mu\Omega$ cm/at. %.[4] The large difference from the O resistance determined in the present work occurs even though the two species have the same valence. Valence is ordinarily the main factor in determining residual resistance.

Equally large differences appear in the optical spectra. Figure 11 presents spectra for Te in Cs that reveal normalized absorption cross sections a factor of 20 larger than those for O in the accessible energy range. Te clearly resembles I and Xe in that it possesses well-defined transitions between local configurations having ionic characters. An interpretation of these data must, however, await an extension of the measurements to lower photon energy where the persistent Te threshold presumably occurs. Still larger effects are expected for oxygen in the energy range below 5 eV, in order that the f sum rule be satisfied, but these, also, must await investigations using other techniques.

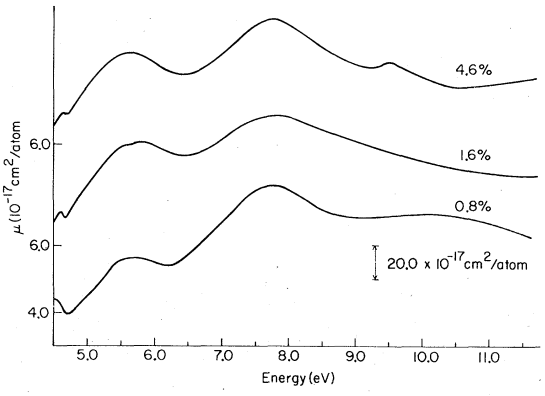

FIG. 11. Absorption spectra of tellurium in Cs.

IV. DISCUSSION

A detailed discussion of the assembled data would be out of place here since there exist neither theoretical models of the structures of O and H in alkali metals, not the theoretical base from which to interpret the experimental resistances or optical spectra. The present comments will therefore mainly concern the clear evidence that both O and H remain on interstitial sites of the alkali metals.

One major aspect of the evidence concerns the impurity-induced resistivity. For H and O the observed impurity resistance is almost an order of magnitude less than typical values for substitutional impurities in these hosts, and for the isovalent species Te in particular. The values are, in fact, rather typical of these impurities as interstitial atoms in transition metals. In Pd and Ti, for example, interstitial H introduces resistivities of 0.4 and 0.5 $\mu\Omega$ cm/at. %, respectively.[13,14] As an approximate guide in the interpretation of such small resistances we can quote the Born approximation[15] to the H phase shift in vacuum:

$$\eta_0 = (me^2/2k_F\hbar^2)[\ln(1+k_F^2a_0^2) + k_F^2a_0^2/(1+k_F^2a_0^2)],$$

which leads to an estimated resistance 0.7 $\mu\Omega$ cm/at. % in K, Rb, and Cs. Clearly, these results are consistent in order of magnitude with scattering of plane waves near k_F by the hydrogenic state. It is likely that interstitial H in alkali metals would indeed possess a structure rather resembling atomic H.

In both the cases of H and O in alkali hosts the spectra reveal observable presistent features that appear to vary systematically from one host to the next. Both sets of spectra are notably independent of impurity-impurity interaction effects, since the normalized H spectra appear generally insensitive to composition for $c \lesssim 30$ at. % and the O spectra for $c \lesssim 15$ at. %.

The most interesting feature of the optical data is the sharp peak near 11.5 eV induced in the Cs spectrum by *both* H and O. This prominent effect has been established unambiguously despite its proximity to the LiF cutoff. It is absent for these impurities in other hosts and for substitutional impurities in Cs also. It is evidently an explicit signature of the interstitial location of H and O

in the Cs lattice.

The most likely explanation of this remarkable effect is that interstitial impurities are forced into close contact with neighboring host cores. The repulsive energy raises the core states and thus lowers the core excitation energy. This explains why H and O should lead to similar optical effects in the same spectral region because it is a *host* excitation that becomes perturbed. The differing *magnitudes* of the effects for H and O arise from their dissimilar interactions with the neighboring cores. It also explains why the effect occurs for the Cs host alone. Only for the Cs 0_{23} excitations can a small interstitial-induced red shift displace the host core excitation from its unperturbed location at ~11.8 eV into the energy range accessible to our measurements.[12] Its presence in the doped sample, and absence in the pure, introduces a derivative structure into the present differential measurements. We expect that similar phenomena will be discovered for other alkali-metal hosts on the red edge of their outer core excitation spectra in interstitial alloys. If confirmed, this novel effect may possibly become established as a reliable monitor of interstitial site occupancy by impurities in metals.

In concluding this report we note that H-induced changes in transition-metal spectra have been interpreted by other workers as originating in band-structure effects.[16] The present work casts new light on this interpretation. It is possible that the observed spectral shifts in these cases also originate rather directly in hydrogen-induced shifts of the transition-metal *d* excitations.

ACKNOWLEDGMENTS

This work was supported by the NSF through the University of Illinois MRL Grant No. DMR-77-23999 and by ONR through Contract No. N-00014-75-C-0918.

---

*Present address: Naval Medical Research Institute, National Naval Medical Center, Bethesda, Md. 20014.

[1]J. Vogl and G. Alefeld, in *Diffusion in Solids* edited by A. S. Nowick and J. J. Burton (Academic, New York, 1975).

[2]Hydrogen in Metals, edited by G. Alefeld and J. Vogl (Springer-Verlag, Berlin, 1978) contains a number of comprehensive reviews concerning both dilute H solutions and hydride phases of transition metals.

[3]W. Rauch, Z. Phys. 111, 640 (1939).

[4]R. Avci and C. P. Flynn, Phys. Rev. Lett. 37, 864 (1976); 41, 428 (1978), and unpublished.

[5]D. J. Phelps, R. A. Tilton, and C. P. Flynn, Phys. Rev. B 14, 5254 (1976).

[6]D. J. Phelps and C. P. Flynn, Phys. Rev. B 14, 5279 (1976).

[7]M. M. Eisenstadt, Rev. Sci. Instrum. 36, 1878(N) (1965).

[8]D. O. Hayward, in *Chemisorption and Reactions on Metallic Films*, edited by J. R. Anderson (Academic, New York, 1971).

[9]J. R. Anderson and I. M. Ritchie, J. Phys. Chem. 11, 3681 (1966).

[10]J. Erskine (private communication) calculated from data provided by W. F. Giauque, J. Res. Natl. Bur. Stand. 52, 4816 (1930).

[11]W. Rauch, Z. Phys. 116, 652 (1940).

[12]T. Ishii, Y. Sakisaka, and S. Yamaguchi, J. Phys. Soc. Jpn. 42, 876 (1977).

[13]W. F. Lindsay, Jr. and F. W. Pement, J. Chem. Phys. 36, 1229 (1962).

[14]See article by J. W. Geus, in *Chemisorption and Reactions on Metallic Films*, edited by J. R. Anderson (Academic, New York, 1971).

[15]N. F. Mott and H. S. W. Massey, *Theory of Atomic Collisions* (Oxford U. P., New York, 1965).

[16]A. C. Switendick, Ber. Bunsunges. Phys. Chem. 76, 535 (1972).